ELectronics EXpress

LETTER

IEICE Electronics Express, Vol.14, No.2, 1–10

A photonic-plasmonic mode converter using mode-coupling-based polarization rotation for metal-inserted silicon platform

Yuhei Ishizaka[1a)], **Masaru Nagai**[2], **Takeshi Fujisawa**[2], **and Kunimasa Saitoh**[2]

[1] *Department of Science and Engineering, Kanto Gakuin University, Yokohama, Japan*

[2] *Graduate School of Information Science and Technology, Hokkaido University, Sapporo, Japan*

a) *ishizaka@kanto-gakuin.ac.jp*

Abstract: We present a photonic-plasmonic mode converter using mode-coupling-based polarization rotation for connecting a silicon wire and hybrid plasmonic waveguides on a metal-inserted silicon platform. By using the polarization rotator based on defect-introduced silicon wire waveguide, the proposed mode converter can convert the photonic TE mode into the hybrid plasmonic TM mode. At the beginning, to identify a cross-sectional structure for polarization conversion, we investigate the hybrid parameters that determine the degree of mode rotation using the two-dimensional vector finite element method. Next, using the three-dimensional vector finite element method, we investigate the conversion characteristics of the whole device including input and output ports. Numerical results show that the extinction ratio of 46 dB and the insertion loss of 0.36 dB are achieved. The tolerance of the defect is also numerically evaluated. Our proposed mode converter can reduce insertion losses compared to conventional mode converters based on a taper-introduced butt joint structure.

Keywords: slot waveguides, plasmonic waveguides, surface plasmon polariton, finite element method

Classification: Integrated optoelectronics

References

[1] S. Zhu, *et al.*: "Components for silicon plasmonic nanocircuits based on horizontal Cu-SiO_2-Si-SiO_2-Cu nanoplasmonic waveguides," Opt. Express **20** (2012) 5867 (DOI: 10.1364/OE.20.005867).

[2] R. M. Briggs, *et al.*: "Efficient coupling between dielectric-loaded plasmonic and silicon photonic waveguides," Nano Lett. **10** (2010) 4851 (DOI: 10.1021/nl1024529).

DOI: 10.1587/elex.13.20160989
Received October 9, 2016
Accepted November 24, 2016
Publicized December 22, 2016
Copyedited January 25, 2017

[3] A. V. Krasavin and A. V. Zayats: "Silicon-based plasmonic waveguides," Opt. Express **18** (2010) 11791 (DOI: 10.1364/OE.18.011791).
[4] M. Z. Alam, *et al.*: "Super mode propagation in low index medium," Proc. Lasers and Electro-Optics (2007) JThD112 (DOI: 10.1109/CLEO.2007.4453278).
[5] R. F. Oulton, *et al.*: "A hybrid plasmonic waveguide for subwavelength confinement and long-range propagation," Nat. Photonics **2** (2008) 496 (DOI: 10.1038/nphoton.2008.131).
[6] D. Dai and S. He: "A silicon-based hybrid plasmonic waveguide with a metal cap for a nano-scale light confinement," Opt. Express **17** (2009) 16646 (DOI: 10.1364/OE.17.016646).
[7] M. Wu, *et al.*: "Conductor-gap-silicon plasmonic waveguides and passive components at subwavelength scale," Opt. Express **18** (2010) 11728 (DOI: 10.1364/OE.18.011728).
[8] Y.-J. Lu, *et al.*: "All-color plasmonic nanolasers with ultralow thresholds," Proc. Lasers and Electro-Optics Pacific Rim (2013) WI4-1 (DOI: 10.1109/CLEOPR.2013.6600140).
[9] L. Gao, *et al.*: "Ultra-compact and low-loss polarization rotator based on asymmetric hybrid plasmonic waveguide," IEEE Photonics Technol. Lett. **25** (2013) 2081 (DOI: 10.1109/LPT.2013.2281425).
[10] J. N. Caspers, *et al.*: "Experimental demonstration of an integrated hybrid plasmonic polarization rotator," Opt. Lett. **38** (2013) 4054 (DOI: 10.1364/OL.38.004054).
[11] L. Sanchez and P. Sanchis: "Broadband 8 μm long hybrid silicon-plasmonic transverse magnetic-transverse electric converter with losses below 2 dB," Opt. Lett. **38** (2013) 2842 (DOI: 10.1364/OL.38.002842).
[12] M. Komatsu, *et al.*: "Compact polarization rotator based on surface plasmon polariton with low insertion loss," IEEE Photon. J. **4** (2012) 707 (DOI: 10.1109/JPHOT.2012.2195650).
[13] N. Zhu and T. Mei: "Analysis of an ultra-compact wavelength filter based on hybrid plasmonic waveguide structure," Opt. Lett. **37** (2012) 1751 (DOI: 10.1364/OL.37.001751).
[14] H.-S. Chu, *et al.*: "Submicrometer radius and highly confined plasmonic ring resonator filters based on hybrid metal-oxide-semiconductor waveguide," Opt. Lett. **37** (2012) 4564 (DOI: 10.1364/OL.37.004564).
[15] S. Zhu, *et al.*: "Experimental demonstration of vertical Cu-SiO2-Si hybrid plasmonic waveguide components on an SOI platform," IEEE Photonics Technol. Lett. **24** (2012) 1224 (DOI: 10.1109/LPT.2012.2199979).
[16] D. Dai, *et al.*: "Silicon hybrid plasmonic submicron-donut resonator with pure dielectric access waveguides," Opt. Express **19** (2011) 23671 (DOI: 10.1364/OE.19.023671).
[17] M. Z. Alam, *et al.*: "Compact and silicon-on-insulator-compatible hybrid plasmonic TE-pass polarizer," Opt. Lett. **37** (2012) 55 (DOI: 10.1364/OL.37.000055).
[18] M. Z. Alam, *et al.*: "Compact low loss and broadband hybrid plasmonic directional coupler," Opt. Express **21** (2013) 16029 (DOI: 10.1364/OE.21.016029).
[19] J. Wang, *et al.*: "Sub-μm^2 power splitters by using silicon hybrid plasmonic waveguides," Opt. Express **19** (2011) 838 (DOI: 10.1364/OE.19.000838).
[20] X. Guan, *et al.*: "Extremely small polarization beam splitter based on a multimode interference coupler with a silicon hybrid plasmonic waveguide," Opt. Lett. **39** (2014) 259 (DOI: 10.1364/OL.39.000259).
[21] J. Chee, *et al.*: "CMOS compatible polarization splitter using hybrid plasmonic waveguide," Opt. Express **20** (2012) 25345 (DOI: 10.1364/OE.20.025345).

DOI: 10.1587/elex.13.20160989
Received October 9, 2016
Accepted November 24, 2016
Publicized December 22, 2016
Copyedited January 25, 2017

[22] R. G. Mote, *et al.*: "Compact and efficient coupler to interface hybrid dielectric-loaded plasmonic waveguide with silicon photonic slab waveguide," Opt. Commun. **285** (2012) 3709 (DOI: 10.1016/j.optcom.2012.04.037).
[23] P. Shi, *et al.*: "Enhanced coupling efficiency between dielectric and hybrid plasmonic waveguides," J. Opt. Soc. Am. B **30** (2013) 1426 (DOI: 10.1364/JOSAB.30.001426).
[24] Y. Song, *et al.*: "Broadband coupler between silicon waveguide and hybrid plasmonic waveguide," Opt. Express **18** (2010) 13173 (DOI: 10.1364/OE.18.013173).
[25] T. Tsuchizawa, *et al.*: "Microphotonics devices based on silicon microfabrication technology," IEEE J. Sel. Top. Quantum Electron. **11** (2005) 232 (DOI: 10.1109/JSTQE.2004.841479).
[26] S. Kim and M. Qi: "Polarization rotation and coupling between silicon waveguide and hybrid plasmonic waveguide," Opt. Express **23** (2015) 9968 (DOI: 10.1364/OE.23.009968).
[27] Y.-J. Chang and T.-H. Yu: "Photonic-quasi-TE-hybrid-plasmonic-TM polarization mode converter," J. Lightwave Technol. **33** (2015) 4261 (DOI: 10.1109/JLT.2015.2464685).
[28] Z. Wang and D. Dai: "Ultrasmall Si-nanowire-based polarization rotator," J. Opt. Soc. Am. B **25** (2008) 747 (DOI: 10.1364/JOSAB.25.000747).
[29] K. Saitoh and M. Koshiba: "Full-vectorial imaginary-distance beam propagation method based on a finite element scheme: application to photonic crystal fibers," IEEE J. Quantum Electron. **38** (2002) 927 (DOI: 10.1109/JQE.2002.1017609).
[30] Y. Ishizaka, *et al.*: "Three-dimensional finite-element solutions for crossing slot-waveguides with finite core-height," J. Lightwave Technol. **30** (2012) 3394 (DOI: 10.1109/JLT.2012.2217478).
[31] P. B. Johnson and R. W. Christy: "Optical constants of the noble metals," Phys. Rev. B **6** (1972) 4370 (DOI: 10.1103/PhysRevB.6.4370).
[32] V. P. Tzolov and M. Fontaine: "A passive polarization converter free of longitudinally-periodic structure," Opt. Commun. **127** (1996) 7 (DOI: 10.1016/0030-4018(96)00039-9).
[33] A. Melikyan, *et al.*: "Photonic-to-plasmonic mode converter," Opt. Lett. **39** (2014) 3488 (DOI: 10.1364/OL.39.003488).

1 Introduction

Plasmonic waveguides have been attracted as future dense electronic-photonic chips owing to the usefulness of compact bends and splitters [1] due to the strong light confinement. So far, dielectric-loaded surface plasmon polariton waveguides (DLSPPWs) [2, 3] and hybrid plasmonic waveguides (HPWs) [4, 5, 6, 7], have been proposed. DLSPPWs are constructed by bonding a dielectric waveguide to a metal substrate. On the other hand, HPWs have a slotted silica layer that is sandwiched between a metal material and a silicon wire waveguide. Generally, HPWs have the advantage of the long propagation length compared with DLSPPWs due to their low loss. Therefore, HPWs are used in several applications, such as an optical laser [8], polarization rotators [9, 10, 11, 12], a wavelength filter [13], ring resonators [14, 15, 16], an optical polarizer [17], a directional coupler [18], a power splitter [19], and polarization splitters [20, 21]. Since these plasmonic devices are fabricated on Si substrate together with optical devices based on silicon

DOI: 10.1587/elex.13.20160989
Received October 9, 2016
Accepted November 24, 2016
Publicized December 22, 2016
Copyedited January 25, 2017

wire waveguides, the coupling between these two different waveguides are necessary for their integration. Hereafter, an optical mode confined in silicon wire waveguides by total internal reflection is called 'photonic mode' and in plasmonic waveguides by surface plasmon polariton is called 'plasmonic mode'. To efficiently integrate these devices with silicon photonic waveguides, transmission-efficient photonic-plasmonic mode converters to couple plasmonic waveguides and silicon photonic waveguides are required. In response to the requirement, various couplers for connecting a silicon wire waveguide and an HPW [22, 23, 24] have been proposed. The reported devices convert the photonic TM mode to the plasmonic TM mode. From the practical point of view, however, the TE mode is frequently used in silicon wire waveguides due to their low bending losses [25] although the TM plasmonic mode is used in HPWs. To adapt such a situation, mode converters using mode-evolution-based polarization rotation for converting photonic TE mode to plasmonic TM mode have been reported [26, 27]. In [26], coupling efficiency of the mode-coupling-based mode converter with metal cap structure, i.e., metal layer is put on an upper part of the silicon core, has been also investigated. In contrast, coupling efficiency when introducing mode-coupling-based polarization rotation has not been investigated for metal-inserted silicon platform [22], i.e., metal layer is placed at the bottom of the silicon core.

In this paper, we propose a photonic-plasmonic mode converter using a mode-coupling-based polarization rotation for metal-inserted silicon platform. Our proposed mode converter can smoothly convert the photonic TE mode of the silicon wire waveguide into the plasmonic TM mode of the HPW by using the polarization rotation induced by an asymmetric waveguide geometry [28], which is our novelty. First, we estimate the degree of polarization rotation of the asymmetrical HPW using the two-dimensional (2-D) vector finite element method (VFEM) [29]. Next, by applying the three-dimensional (3-D) VFEM for the waveguide discontinuity problem [30] to the whole device structure including input and output ports, we evaluate the extinction ratio and the insertion loss. Numerical results show that the maximum extinction ratio of 46 dB and a low insertion loss of 0.36 dB are obtained. For the wavelength from 1.53 μm to 1.57 μm, the extinction ratio is higher than 20 dB and the insertion loss is lower than 0.6 dB. Finally, we compare the proposed photonic-plasmonic mode converter with the reported photonic-plasmonic mode converters.

2 Mode conversion efficiency

Fig. 1 shows a schematic of a photonic-plasmonic mode converter based on a polarization rotation for connecting a silicon wire waveguide and an HPW. In the proposed device, the photonic TE mode is launched into an input port and converted to the plasmonic TM mode at an output port. A defect at the corner of the silicon waveguide is introduced to rotate the polarization. Under the silicon wire waveguide with the defect and the thin SiO_2 layer, a metal is placed to form hybrid plasmonic structure. Typically, aluminium [3], silver [5, 6], gold [7], and copper [1] are used in plasmonic waveguides. In this paper, we choose silver as the metal material [24]. Over cladding material is air. We assume that the refractive indexes

DOI: 10.1587/elex.13.20160989
Received October 9, 2016
Accepted November 24, 2016
Publicized December 22, 2016
Copyedited January 25, 2017

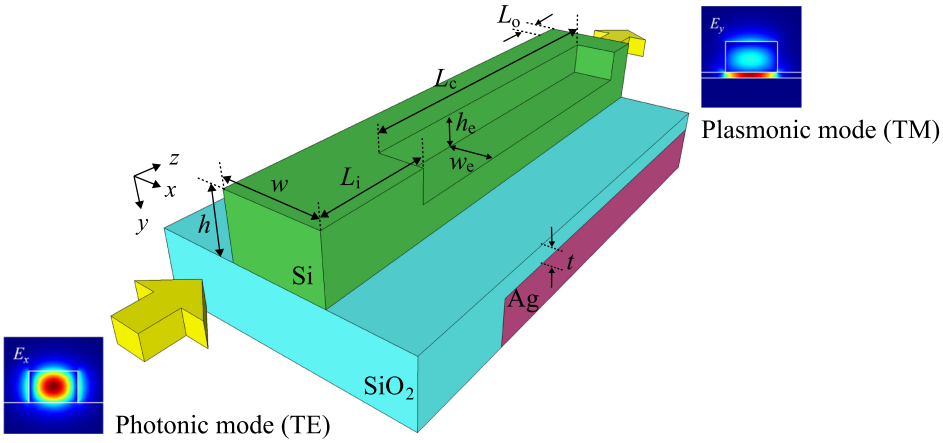

Fig. 1. Schematic of a photonic-plasmonic mode converter based on a polarization rotation. The defect is introduced at the upper corner of the silicon wire waveguide. In the converter, the photonic TE mode (left inset) is inputted and the plasmonic TM mode (right inset) is outputted.

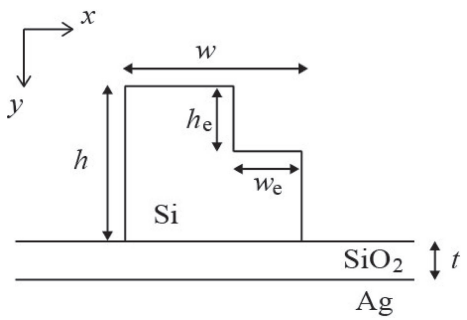

Fig. 2. Cross-sectional view of the photonic-plasmonic mode converter.

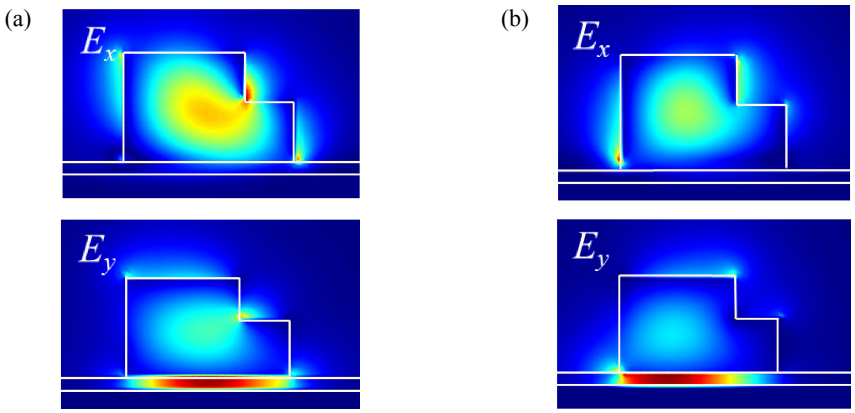

Fig. 3. Electric field distributions of (a) the 1st hybrid and (b) the 2nd hybrid modes for $h = 0.3$ µm, $w = 0.5$ µm, $h_e = 0.15$ µm, $w_e = 0.13$ µm, and $t = 0.05$ µm at the wavelength of 1.55 µm. For the 1st and the 2nd hybrid modes, the E_x element is mainly confined in the silicon core, and the E_y element is strongly confined in the silica layer.

of Si, SiO_2, Air, and Ag are 3.48, 1.45, 1.0, and $0.145 - j11.359$ [31], respectively. The lengths of the straight input silicon wire waveguide and the output HPW, L_i and L_o, are set to 1 µm. We denote the waveguide width, the waveguide height, and

DOI: 10.1587/elex.13.20160989
Received October 9, 2016
Accepted November 24, 2016
Publicized December 22, 2016
Copyedited January 25, 2017

the SiO_2-thickness as w, h, and t, respectively. In all cases, we chose $h = 0.3\,\mu m$, $w = 0.5\,\mu m$, and $t = 0.05\,\mu m$ as a design example. The length of polarization rotation section is defined as L_c. In addition, the defect width and height are denoted as w_e and h_e, respectively. Fig. 2 shows a cross-sectional view of the photonic-plasmonic mode converter based on the HPW. For this 2-D structure, we investigate the waveguide parameters that can efficiently rotate the polarization. The wavelength is fixed to 1.55 µm. To investigate the efficiency of mode conversion, we evaluated the hybrid parameter R for different defect width and height. By setting the defect at the corner of the silicon core waveguide, the optical axis of the silicon core waveguide is slanted, and two hybrid supermodes called '1st hybrid mode' and '2nd hybrid mode' are excited. The 1st hybrid mode has a larger effective index than the 2nd hybrid mode. Figs. 3(a) and (b) show the electric field distributions of the 1st and the 2nd hybrid modes, respectively, for $h_e = 0.15\,\mu m$, $w_e = 0.13\,\mu m$. From Fig. 3, we can see that the E_x element is mainly confined in the silicon core and the E_y element is strongly confined in the silica layer for both 1st and 2nd hybrid modes. To estimate the ratio between the E_x and the E_y elements for the 1st or the 2nd hybrid mode, the hybrid parameter R is given by [32]:

$$R = \frac{\iint n^2(x,y)E^2_{\text{minor}}(x,y)dxdy}{\iint n^2(x,y)E^2_{\text{major}}(x,y)dxdy}, \quad 0 \le \mathrm{R} \le 1, \tag{1}$$

where $n(x, y)$ is the refractive index distribution, E_{minor} and E_{major} are the minor and major electric field components (E_x or E_y). The maximum of R is 1 and the larger value of R is better in terms of polarization rotation. Hereafter, the hybrid parameter for the 1st hybrid mode is R_1, and for the 2nd hybrid mode is R_2. Figs. 4(a) and (b) show R_1 and R_2, respectively. From Fig. 4, we can see belt-like distributions for both the 1st and 2nd hybrid modes. And, the positions of the belts are slightly different between the 1st and the 2nd hybrid mode. To analyze the 3-D structure including the input and output ports, w_e adopt one defect structure that has $h_e = 0.15\,\mu m$ and $w_e = 0.13$, at which both R_1 and R_2 are close to 1. In this case, R_1 and R_2 are 0.83 and 0.86, respectively. An optical mode is rotated from the TE mode to the TM mode by propagating the half beat length. Here, the half beet length, L_π, is given by the following equation [32]:

$$L_\pi = \frac{\pi}{|\beta_1 - \beta_2|} \tag{2}$$

where β_1 and β_2 are the propagation constants of the 1st and 2nd hybrid modes. The calculated half beet length is 6.3 µm.

3 3-D analysis and discussion

To investigate the conversion characteristics of the photonic-plasmonic mode converter, we evaluate the extinction ratio and the insertion loss of the photonic-plasmonic mode converter based on the polarization rotation (Fig. 1) using the 3-D VFEM. The wavelength is 1.55 µm except for the analysis of the wavelength dependence. In the 3-D simulation, the photonic TE mode is inputted (see Fig. 1)

DOI: 10.1587/elex.13.20160989
Received October 9, 2016
Accepted November 24, 2016
Publicized December 22, 2016
Copyedited January 25, 2017

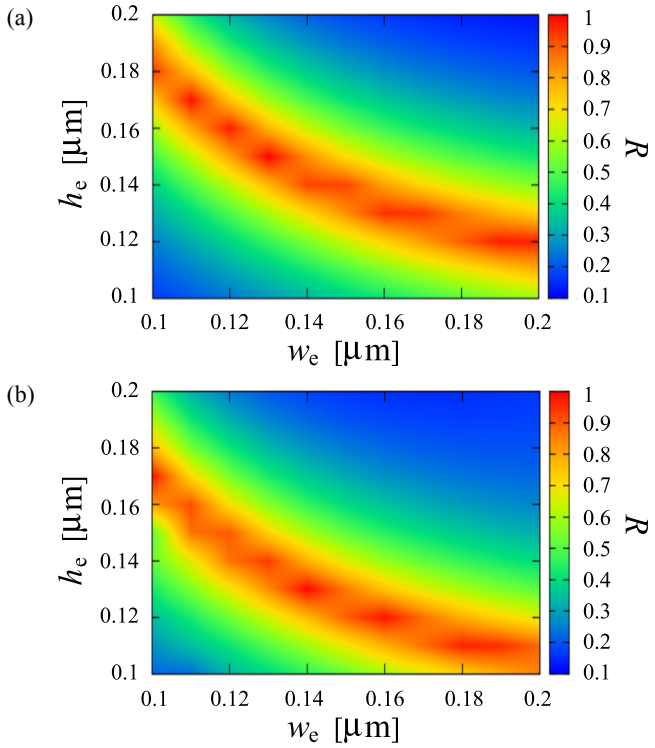

Fig. 4. Hybrid parameters for (a) the 1st and (b) the 2nd hybrid modes for $h = 0.3$ μm, $w = 0.5$ μm, and $t = 0.05$ μm. The belt-like distributions are shown for both the 1st and 2nd hybrid modes. The position of the belts is a slightly different between the 1st and the 2nd hybrid modes.

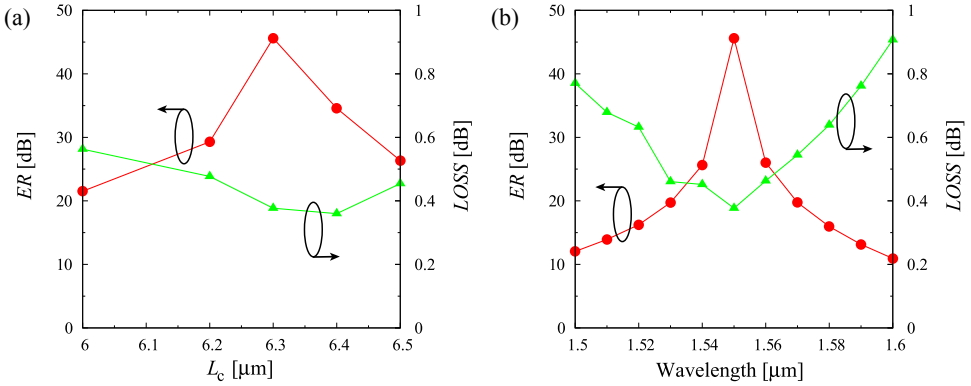

Fig. 5. (a) The extinction ratio and the insertion loss as a function of L_c for $h_e = 0.15$ μm and $w_e = 0.13$ μm. (b) The extinction ratio and the insertion loss as a function of the wavelength from 1.5 μm to 1.6 μm (the parts of C and L bands) for $h_e = 0.15$ μm, $w_e = 0.13$ μm, and $L_c = 6.3$ μm.

and the input power is normalized as 1. The extinction ratio, ER [dB], is obtained by the following equation [12]:

$$ER = 10 \log_{10} \frac{P_{TM}}{P_{TE}} \tag{3}$$

where P_{TM} and P_{TE} are the normalized transmission power at the output port of the rotated mode (plasmonic TM mode of the HPW) and the unrotated mode (photonic

DOI: 10.1587/elex.13.20160989
Received October 9, 2016
Accepted November 24, 2016
Publicized December 22, 2016
Copyedited January 25, 2017

TE mode), respectively. The insertion loss, *LOSS* [dB], is obtained by the following equation [12]:

$$LOSS = -10\log_{10} P_{\mathrm{TM}} \tag{4}$$

Fig. 5(a) shows the extinction ratio and the insertion loss as a function of L_c for $h_e = 0.15\,\mu\mathrm{m}$ and $w_e = 0.13\,\mu\mathrm{m}$. From Fig. 5(a), we can see that the maximum *ER* of 46 dB and the lowest *LOSS* of 0.36 dB are obtained when $L_c = 6.3\,\mu\mathrm{m}$. The obtained result of the device length is in good agreement with the half beat length calculated by Eq. (2). Fig. 5(b) shows the extinction ratio and the insertion loss as a function of the wavelength from 1.5 µm to 1.6 µm (the parts of C and L bands) for $h = 0.3\,\mu\mathrm{m}$, $w = 0.5\,\mu\mathrm{m}$, and $t = 0.05\,\mu\mathrm{m}$. We can see that *ER* is larger than 20 dB in the range from 1.53 µm to 1.57 µm, and *ER* is larger than 10 dB in the range from 1.5 µm to 1.6 µm. In addition, *LOSS* is lower than 0.6 dB in the range from 1.53 µm to 1.57 µm, and *LOSS* is lower than 1 dB in the range from 1.5 µm to 1.6 µm. To investigate the defect design tolerance, we evaluate *ER* and *LOSS* when h_e and w_e are changed from 0.15 and 0.13 µm. The differences in height and width are Δh_e and Δw_e. Figs. 6(a) and (b) show the extinction ratio and the insertion loss with respect to Δh_e and Δw_e. From Fig. 6, it is recognized that *ER* is higher than 15 dB even if $|\Delta h_e| = 10\,\mathrm{nm}$, and *LOSS* does not exceed 1 dB even if $|\Delta w_e| = 20\,\mathrm{nm}$.

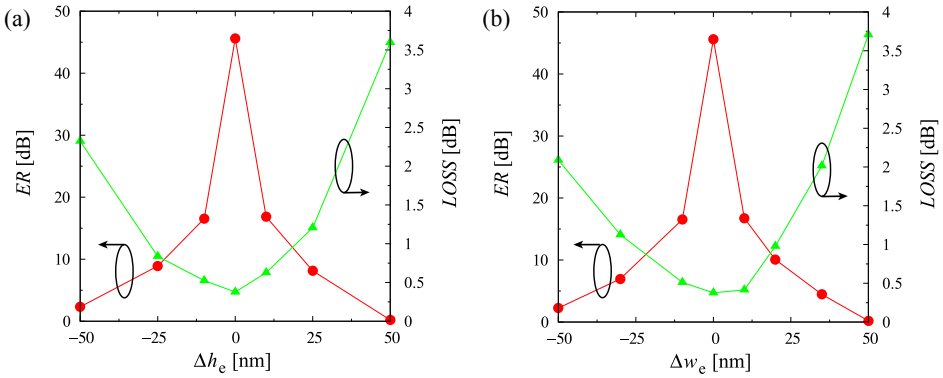

Fig. 6. The extinction ratio and the insertion loss as a function of (a) Δh_e and (b) Δw_e, where Δh_e is the misalignment from $h_e = 0.15\,\mu\mathrm{m}$ and Δw_e is the misalignment from $w_e = 0.13\,\mu\mathrm{m}$.

We compare the proposed mode converter with various types of reported mode converters in terms of the insertion loss (or the transmittance) and the device length. The comparisons for the insertion loss and device length are summarized in Table I. The converter reported in [2] has a taper waveguide to couple the photonic TM mode to the plasmonic TM mode in the DLSPPW. The converters reported in [7, 15, 22, 23] and [24] have a taper structure to couple the photonic TM mode to the plasmonic TM mode in the HPW. The metal layer is put on an upper part of the silicon core in the converters of [7, 15, 23] and [24], while the metal layer is placed at the bottom of the silicon core in the converter [22]. The converter reported in [33] uses a directional coupler composed of silicon wire and MIM waveguides. From Table I, we can see that our proposed photonic-plasmonic mode converter is

DOI: 10.1587/elex.13.20160989
Received October 9, 2016
Accepted November 24, 2016
Publicized December 22, 2016
Copyedited January 25, 2017

superior to others in terms of the transmittance (the insertion loss) except for [23]. Although the transmittance of our converter is slightly lower than the converter proposed in [23], our converter can use the TE mode as the input mode in silicon wire waveguides. In silicon wire waveguides, the TE mode is mainly used because the bending loss of the TE mode is lower than that of the TM mode [25]. Meanwhile, we adopt the same approach reported by [26, 27] in terms of polarization rotation, but the position of the metal layer of our converter is largely different from the conventional structures. In addition, a higher coupling efficiency can be achieved compared with the conventional polarization-rotation-based mode converters [26, 27]. From the above discussion, it is considered that our proposed photonic-plasmonic mode converter can indicate the superiority for metal-inserted silicon platform.

Table I. Comparisons between the conventional photonic-plasmonic mode converters and our device.

Photonic-plasmonic mode converters	Conversion mechanism	Transmittance [%]	Device length [μm]	Input mode – Output mode
This work	Polarization rotation (mode coupling)	92 (simulation)	6.3	TE – TM
[2]	Taper	79 ± 2 (experiment)	Not mentioned	TM – TM
[7]	Taper	88 (simulation) and 80 (experiment)	1	TM – TM
[15]	Taper	87 (simulation) and 86 (experiment)	1	TM – TM
[22]	Taper	80 (simulation)	0.4	TM – TM
[23]	Taper	94.4 (simulation)	0.4	TM – TM
[24]	Taper	70 (simulation)	0.4	TM – TM
[26]	Polarization rotation (mode coupling/evolution)	<78% (simulation)	4.5	TE – TM
[27]	Polarization rotation (mode evolution)	88.8% (simulation)	<7	TE – TM
[33]	Directional coupler	85 (simulation)	2.6	TM – TM

4 Conclusion

We proposed a photonic-plasmonic mode converter using mode-coupling-based polarization rotation for metal-inserted silicon platform. Because the input mode of the proposed mode converter is the frequently-used TE mode, it is convenient for integrating silicon wire and plasmonic waveguides. Through the polarization rotation, the plasmonic TM mode is efficiently excited in the HPW-based circuit. To identify the cross-sectional structure, using the 2-D VFEM, we investigated the hybrid parameter and found the structure with large R. After evaluating the hybrid parameter and the half beat length, we investigated the extinction ratio and the

DOI: 10.1587/elex.13.20160989
Received October 9, 2016
Accepted November 24, 2016
Publicized December 22, 2016
Copyedited January 25, 2017

insertion loss of the whole device including the input and output ports using the 3-D VFEM for the waveguide discontinuity problem. Numerical results showed that the extinction ratio of 46 dB, the insertion loss of 0.36 dB, and the device length of 6.3 μm are obtained. Our proposed mode converter can be useful for a connecting device for future hybrid circuits composed of silicon wire waveguides and HPWs.

DOI: 10.1587/elex.13.20160989
Received October 9, 2016
Accepted November 24, 2016
Publicized December 22, 2016
Copyedited January 25, 2017